Celal Bayar University Journal of Science

A Sensitive Electrochemical Approach for Monitoring Lead in Fish Liver

Ahmet Kaya[1], Canan Onac[1,2*]

[1]Pamukkale University, Department of Chemistry, 20170 Denizli, Türkiye
[2]Pamukkale University, Advanced Technology Application and Research Center, 20170 Denizli, Türkiye
* conac@pau.edu.tr
* Orcid No: 0000-0003-3799-3678

Received: June 12, 2025
Accepted: October 13, 2025
DOI: 10.18466/cbayarfbe.1718352

Abstract

This study presents the development and optimization of a simple, unmodified screen-printed electrode (SPE) method for the electrochemical detection of lead Pb(II), ions using cyclic voltammetry (CV). Key experimental parameters, including the type and concentration of supporting electrolyte and scan rate, were systematically evaluated to enhance the analytical performance of the sensor. Among the electrolytes tested, 0.1 M potassium chloride (KCl) provided the highest peak current and best-defined redox features, while a scan rate of 75 mV/s offered optimal peak resolution and sensitivity. Analytical figures of merit demonstrated a linear detection range of 0.25–10.0 mM, a limit of detection (LOD) of 0.096 mM. The proposed method was successfully applied to fish liver tissue (*Mugil cephalus)*, showing consistent recoveries of 97.16-115.08%. This study presents a simple and cost-effective approach, achieved without the need for nanomaterial enhancements or surface modifications. This study also aims to evaluate the performance of the SPE in detecting Pb(II) in fish liver samples, comparing its sensitivity and accuracy to Inductively Coupled Plasma Optical Emission Spectrometry (ICP-OES). It demonstrates the viability of using unmodified SPEs for reliable Pb(II) detection in complex matrices, providing a practical alternative for environmental and biological monitoring applications.

Keywords: Cyclic voltammetry (CV), electrochemical sensor, fish liver tissue, lead detection, screen-printed electrode (SPE).

1. Introduction

The rapid pace of urbanization and industrial development has significantly contributed to the release and accumulation of heavy metals in the environment, posing serious threats to both human health and ecological balance. These toxic elements, including cadmium (Cd), lead (Pb), mercury (Hg), zinc (Zn), and copper (Cu), often enter the food chain through contaminated water, soil, and air, eventually making their way into the food supply [1,2]. Once introduced into the environment, heavy metals can bioconcentrate in living organisms, leading to long-term exposure even at low concentrations [3]. This persistent accumulation is particularly concerning because it can result in unpredictable and often irreversible health effects [4].

Lead Pb(II), a naturally occurring heavy metal, has played a central role in human history due to its desirable physical properties such as malleability, low melting point, and high density [5]. These characteristics made it useful in a range of ancient and modern applications, from Roman plumbing and cookware to modern batteries and paints [6]. However, despite its historical utility, lead is now widely recognized as a potent environmental toxicant with no safe level of exposure [7]. It poses a particularly grave threat to vulnerable populations like children and pregnant women, where even minimal exposure can result in irreversible developmental and neurological harm [8]. Among the various exposure pathways, water contamination is particularly concerning because it constitutes a direct route for human ingestion and is the primary medium through which aquatic organisms are exposed to lead [9].

In response, regulatory agencies such as the U.S. Environmental Protection Agency (EPA) have established a Maximum Contaminant Level Goal (MCLG) of 0 ppb for lead in drinking water, reflecting the consensus that no level of lead exposure is considered safe [10]. However, due to the complexities of plumbing infrastructure, especially the contribution of lead

leaching from household pipes and fixtures, an enforceable Action Level (AL) of 15 ppb is applied. Exceeding this level in more than 10% of sampled homes triggers mandatory remediation efforts [11].

For aquatic life, the EPA's recommended water quality criteria for lead are hardness-dependent, with lower thresholds in softer water due to increased bioavailability and toxicity. In freshwater systems, chronic exposure limits can be as low as 2.5 μg/L, while in saltwater environments, the chronic criterion is 8.1 μg/L [12].

These environmental limits are particularly important given the role of aquatic organisms, especially fish, in both ecosystems and human diets [13]. Fish are widely regarded as one of the healthiest and most nutrient-dense food sources due to their high-quality protein content and a broad spectrum of essential nutrients, including vitamins and minerals vital for enzymatic activity and physiological growth [14].

However, their role in the food chain also makes them susceptible to environmental pollutants, particularly heavy metals like lead. Fish accumulate lead primarily through two pathways: direct absorption from contaminated water via their gills and indirect ingestion through their diet [15].

The liver, an organ central to metabolism and detoxification in fish, is particularly prone to accumulating lead [16]. This makes the liver a key target tissue for monitoring the presence of environmental contaminants. Detecting and quantifying lead in fish liver is crucial for several reasons. First, it provides an accurate reflection of the level of contamination in aquatic ecosystems since fish serve as effective bioindicators of water quality [17]. Second, it plays a vital role in food safety and public health, as fish are a major component of human diets in many parts of the world [18]. Therefore, systematic monitoring of lead concentrations in fish, particularly in liver tissues, is essential for assessing environmental pollution, setting regulatory safety limits, and protecting both ecosystem and human health.

Traditional analytical techniques for the detection of heavy metals, such as Atomic Absorption Spectroscopy (AAS), Inductively Coupled Plasma Mass Spectrometry (ICP-MS), and Inductively Coupled Plasma Optical Emission Spectrometry (ICP-OES), are widely acknowledged for their high sensitivity, accuracy, and reliability. These methods are frequently used in environmental monitoring, food safety, and clinical diagnostics [19, 20]. Despite their analytical advantages, these techniques come with significant limitations. They require highly sophisticated and costly instrumentation, as well as complex, labor-intensive sample preparation protocols that often involve digestion or extraction steps under controlled laboratory conditions. Moreover, the operation and interpretation of data generated by these instruments require trained personnel with specialized expertise. These requirements not only increase the overall cost and time analysis but also limit the feasibility of deploying these methods for real-time or on-site applications. In most cases, samples must be collected in the field and transported to centralized laboratories, further delaying the detection process and potentially compromising sample integrity.

As a result, there is a growing interest in developing alternative, low-cost, and portable analytical approaches that can provide rapid and reliable detection of heavy metals directly at the point of need.
In light of the limitations associated with conventional analytical techniques, electrochemical sensors have emerged as a promising and practical alternative for the detection of heavy metals. These sensors offer several key advantages that make them particularly suitable for real-time, on-site monitoring applications. Their high sensitivity and rapid response times enable the detection of trace levels of toxic metals with minimal delay, while their portability and cost-effectiveness allow for decentralized testing outside of traditional laboratory settings. Unlike traditional methods, which often require complex sample preparation and expensive instrumentation, electrochemical sensors can be fabricated from low-cost materials, such as carbon-based or SPEs, and are generally simpler to operate [21-23]. This makes them especially attractive for use in resource-limited environments and for large-scale environmental or food safety monitoring.

This study presents a simple and effective electrochemical approach for the detection of Pb(II) using a SPE and comparing this approach with ICP-OES. Through systematic optimization of supporting electrolyte type and concentration, as well as scan rate, the method achieves high sensitivity, clear peak resolution, and reliable quantification without requiring complex surface modifications or nanomaterial enhancements. The SPE method provides a simpler and faster approach for detecting Pb(II) in fish (*Mugil cephalus)* liver samples, reducing the need for the more complex and time-consuming sample preparation required by ICP-OES. Moreover, the cost-effectiveness of the electrochemical technique compared to ICP-OES could encourage broader adoption in monitoring programs, improving accessibility to food and environmental safety efforts.

2. Materials and Methods

2.1. Materials

Sodium acetate (CH_3COONa, purity > 99%, Sigma-Aldrich), acetic acid (CH_3COOH, purity > 99%, Sigma-Aldrich), potassium nitrate (KNO_3, purity > 99%, Sigma-Aldrich), phosphate-buffered saline (PBS) tablet, pH

7.2–7.6 (Sigma–P4417), ethanol (C_2H_6O, purity > 99.99%, IsoLab), potassium ferrocyanide ($K_4Fe(CN)_6 \cdot 3H_2O$, purity > 98%, Sigma-Aldrich), potassium ferricyanide ($K_3Fe(CN)_6$, purity > 99%, Sigma-Aldrich), boric acid (H_3BO_3, purity > 99.55%, Sigma-Aldrich), phosphoric acid (H_3PO_4, purity > 99%, Sigma-Aldrich), potassium hydrogen phosphate (K_2HPO_4, purity > 99%, Sigma-Aldrich), potassium dihydrogen phosphate (KH_2PO_4, purity > 99%, Sigma-Aldrich), and lead nitrate ($Pb(NO_3)_2$, purity > 99%, Sigma-Aldrich) were employed in this study. All chemicals were of analytical grade and used as received without further purification. Solutions were prepared and diluted using ultra-pure deionized water with a resistivity of 18.2 MΩ·cm obtained from a reverse osmosis system (Human Corp., Seoul, Korea). All experiments were conducted at room temperature.

2.2. Instrumentation

Electrochemical measurements, including CV and square wave voltammetry (SWV) were carried out using a portable potentiostat (DropSens uSTAT I400, Metrohm, Switzerland) connected to SPEs (Methrom, DRP-110-U75, Working electrode material: Carbon, Working electrode diameter: 0.40 cm, Working electrode position: In the middle of the strip, Auxiliary electrode material: Carbon, Reference electrode material: Silver, Contacts material: Silver, Substrate material: Ceramic, Substrate size: Length: 3.38 cm x Width: 1.02 cm, Substrate thickness: 0.05 cm, Working electrode geometric area (cm^2):0.11). The voltammetric analyses were conducted under ambient laboratory conditions as specified by the manufacturer's protocols. CEM MARS-6, microwave digestion system was used for sample preparation of fish (Matthews, NC in USA). Perkin Elmer Optima 2100 DV, Inductively Coupled Argon Plasma-Optical Emission Spectrometer (ICP-OES) was used for spectroscopic determination.

Supporting instrumentation included a digital pH meter with a combined glass calomel electrode (WTW 720, Weilheim, Germany) for accurate pH adjustments. A centrifuge (NF400, Nüve, Turkey) was utilized for sample preparation, while a high-precision balance (XB 220A, Sweden) ensured reliable mass measurements. Thermal treatments were performed in a laboratory oven (FN 055, Nüve, Turkey), and sample mixing was achieved using an orbital shaker (VWR, USA). The concentration of calibration solutions was prepared with ICP-OES standard solutions that were provided from Perkin Elmer.

2.3. Optimization Procedure

In this study, several key analytical parameters were systematically investigated and optimized, including the type and concentration of the supporting electrolyte as well as the scan rate, using a one-variable-at-a-time (OVAT) approach. All measurements were conducted at room temperature. In a typical batch experiment, 15 µL of 0.1 M potassium chloride (KCl) solution containing Pb(II) ions was applied onto the surface of the SPE, followed by CV/SWV analysis. CV measurements were performed within a potential window ranging from 1.0 V to –2.0 V, using a step size of 2 mV and a scan rate of 50 mV/s. Each experiment was conducted in triplicate to ensure reproducibility. SWV measurements were carried out under the following conditions: the potential was scanned from 0.45 V to –0.15 V, with a step potential of 5 mV and a square wave amplitude of 2 mV. The frequency was set at 20 Hz. Each scan was repeated three times to confirm the reliability and consistency of the results.

2.4. Fish (*Mugil cephalus*) liver sample preparation

Three fish (*Mugil cephalus)* samples were collected from fishermen in Izmir and transported to the laboratory in polyethylene boxes at -4 °C. Upon arrival, the samples were rinsed with distilled water and stored at -80 °C until extraction. 1 g of each fish sample was dried laboratory oven. It was employed solubilization process for liver tissues of each fish samples by microwave digestion system before determination of the samples by electrochemical measurements and ICP-OES. In the One Touch Food approach, 10 mL of HNO_3 and H_2O_2 1:1 (v/v) were added to 0.1 g (wet weight) of liver tissue after it had been weighed. Iprep vessels were used to utilize during digesting. Ramp time of the technique is 30 min at 210°C and the samples keep this temperature for 15 min. The concentration of calibration solutions were 10 µg/kg, 50 µg/kg, 100 µg/kg, 250 µg/kg, and 500 µg/kg, respectively.

3. Results and Discussion

3.1. Electrolyte Type

The choice of supporting electrolyte, including both its ionic constituents and solvent composition, plays a critical role in defining the redox behaviour of metal ions. This influence arises from factors such as complexation effects and the electrolyte's impact on the stability of the electrode surface. An ideal electrolyte should enhance sensitivity by producing high peak currents, offer well-defined and reproducible redox peaks, maintain a low background current and noise level, and exhibit minimal interfering electrochemical activity.

To identify the most suitable supporting electrolyte for Pb(II) detection, four different electrolytes were evaluated: 0.1 M acetate buffer (pH 4.0), 0.1 M KCl, 0.1 M KNO_3, and 0.1 M PBS (pH ~ 7.4). The results, showen in Figure 1, show notable differences in electrochemical performance. Among them, the acetate buffer generated the highest oxidation peak current (1514 µA) at around -0.3 V. It also exhibited a distinct reduction peak current

of 584 µA. However, despite these strong signals, acetate buffer showed a considerably high background current and pronounced capacitive behavior, especially at more negative potentials, which can interfere with sensitive measurements and reduce signal clarity.

PBS yielded the poorest performance, showing a very low oxidation peak current (23 µA) and no clearly defined reduction peak, indicating minimal electrochemical activity. This weak response may be attributed to low ionic strength or unfavorable interactions between the PBS components and Pb(II), rendering it unsuitable for this application. Both KNO_3 and KCl exhibited well-separated redox peaks with better-defined voltammetric features. KNO_3 displayed oxidation and reduction peak currents of 1243 µA and -530 µA, respectively, while KCl showed slightly higher values, 1244 µA for oxidation and -699 µA for reduction, indicating a stronger and more reversible electrochemical response. Therefore, 0.1 M KCl was selected as the optimal supporting electrolyte for subsequent Pb(II) electrochemical detection due to its balanced performance, higher redox peak currents, and stable background signal.

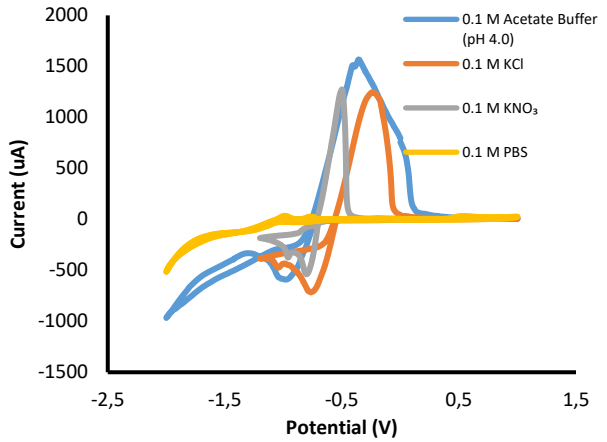

Figure 1. Cyclic voltammograms obtained using different supporting electrolytes. (Pb(II) Concentration: 5 mM; scan range: 1 V to –2 V; step size: 2 mV; scan rate: 50 mV/s).

3.2. Electrolyte Concentration

Electrolyte concentration plays a critical role in determining the quality and reliability of electrochemical measurements, especially in techniques such as voltammetry. One of its primary Electrolyte concentration is crucial in electrochemical measurements like voltammetry, as it reduces solution resistance and minimizes iR drop, preventing distortion of the applied potential. A high supporting electrolyte concentration improves ionic conduction, stabilizes the system, and enhances signal clarity, especially when detecting low-concentration analytes.

The cyclic voltammograms presented in Figure 2 illustrate the electrochemical behavior of Pb(II) in the presence of varying concentrations of KCl: 0.01 M, 0.05 M, 0.1 M, and 0.25 M. As expected, increasing the KCl concentration enhanced the solution conductivity, leading to higher current responses. Among them, 0.25 M KCl exhibited the highest oxidation peak current at 1296 µA and a strongly negative reduction peak at -1263 µA, indicating accelerated electron transfer. However, it showed only a single prominent reduction peak and lacked a second, distinguishable cathodic response. This suggests poor electrochemical resolution, limiting its ability to differentiate multiple lead species or redox transitions.

In contrast, both 0.05 M and 0.1 M KCl solutions produced two well-defined reduction peaks, which are crucial for accurately identifying and quantifying different Pb(II)-related redox processes. Specifically, 0.05 M KCl recorded an oxidation peak of 911 µA, with two distinct reduction peaks at -542 µA and -428 µA. Similarly, 0.1 M KCl demonstrated stronger electrochemical activity with an oxidation peak of 1119 nA, and two clearly resolved reduction peaks at -673 µA and -544 µA. These dual cathodic responses reflect more detailed redox behavior and provide a more complete analytical profile for Pb(II).

Meanwhile, the lowest concentration tested, 0.01 M KCl, exhibited an oxidation peak of 975 nA and a single reduction peak at -607 nA, with the second reduction peak not observed. This limited resolution indicates insufficient support for complex redox activity at low ionic strength.

Overall, 0.1 M KCl emerged as optimal concentration, offering a desirable combination of high signal intensity and superior peak resolution, which ensures both sensitivity and selectivity. Thus, it was selected for subsequent measurements to enable precise and reliable detection of Pb(II).

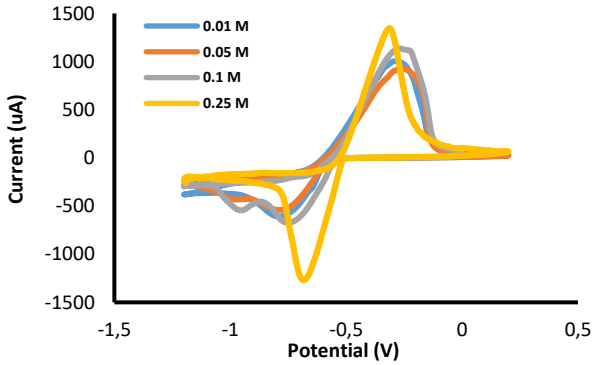

Figure 2. Cyclic voltammograms obtained using different concentration of KCl. (Pb(II) Concentration: 5 mM; scan range: 1 V to –2 V; step size: 2 mV; scan rate: 50 mV/s).

3.3. Scan Rate

The scan rate in CV is a key parameter that affects the shape and features of voltammograms. Varying the scan rate helps assess the kinetics of redox reactions and the analyte's behavior under different conditions. Faster scan rates can reveal intermediate or transient species not seen at slower rates, making scan rate studies crucial for understanding and optimizing electrochemical systems.

The cyclic voltammograms presented in Figure 3 illustrate the electrochemical behavior of a Pb(II) solution at various scan rates ranging from 10 to 500 mV/s. As the scan rate increases, there is a noticeable enhancement in the current response, which is consistent with the expected increase in capacitive and diffusion-controlled processes. At lower scan rates, particularly between 10 and 75 mV/s, two distinct reduction peaks are clearly observable, indicating well-defined and reversible electrochemical reactions. However, as the scan rate exceeds 75 mV/s, the second reduction peak becomes significantly less pronounced. This suggests that at higher scan rates, kinetic limitations hinder the complete redox process, likely due to insufficient time for electron transfer or mass transport. Based on these observations, a scan rate of 75 mV/s was selected as optimal.

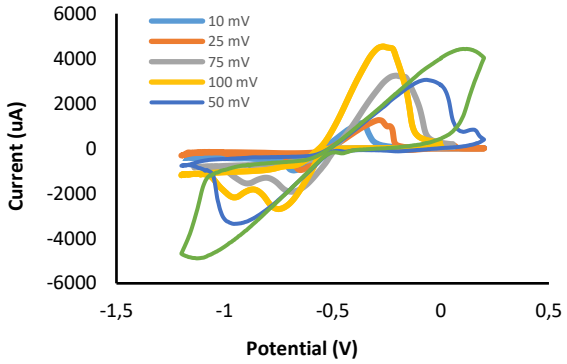

Figure 3. Cyclic voltammograms obtained using different scan rates. (Pb(II) Concentration: 5 mM; scan range: 1 V to –2 V; step size: 2 mV; scan rate: 10 - 500 mV/s).

To clarify the mechanism, the slope of the log ν–log Ip plot was calculated using the experimental data. The obtained slope values were 0.3028 for the anodic peak and 0.3580 for the cathodic peak, which fall within the theoretical range of 0.2–0.6 expected for a diffusion-controlled process. By contrast, values in the range of 0.75–1.0 would indicate a pure adsorption-controlled process [24,25]. Furthermore, the linear regression of the Ip versus $\nu^{1/2}$ plot (Figure 4b) yielded a correlation coefficient (r) of 0.996, which is very close to unity. These results strongly confirm that the controlled electrochemical process is proportional to the square root of the scan rate ($\nu^{1/2}$) as the scan rate increases, the time for diffusion decreases, resulting in a thinner diffusion layer and a steeper concentration gradient of electroactive species at the electrode surface. This higher gradient enhances the flux of species toward the electrode, thereby increasing the current response.

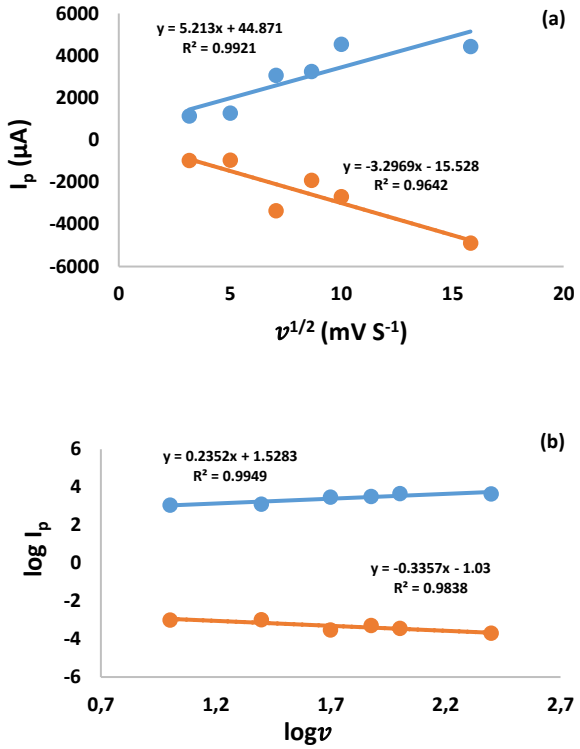

Figure 4. (a) Plot of log anodic and cathodic peak currents versus the log scan rate, (b) Plot of anodic and cathodic peak currents versus the square root of the scan rate.

The increase in peak current with scan rate can be explained by the Randles–Sevcik equation, which states that the peak current (Ip) in a diffusion- electrochemical behavior of copper at the modified electrode is predominantly diffusion-controlled with negligible adsorption effects.

3.4. Analytical figures of merit

The proposed method was evaluated using several key analytical parameters. These included the determination of the linear range for the calibration curves, assessed using Mandel's test for Pb(II) at a 95% confidence level. The limits of detection (LOD) and quantification (LOQ) were calculated under the calibration conditions using 15 blank water samples (N = 15). Furthermore, LOD and LOQ values were independently verified by analyzing the signal-to-noise (S/N) ratios, corresponding to 3σ for LOD and 10σ for LOQ. The results obtained for Pb(II) are summarized in Table 1.

Matrix effects (ME) were evaluated using Eq. (1) by

Celal Bayar University Journal of Science
Volume 21, Issue 4, 2025, p 172-181
Doi: 10.18466/cbayarfbe.1718352

comparing the slopes of the calibration curves prepared in the real (matrix) solution and in the standard (solvent) solution.

$$ME\ (\%) = 100 \times \left(\frac{k_a}{k_b} - 1\right) \quad (1)$$

where k_a is the slope of the matrix-matched calibration and k_b is the slope of solvent calibration. Figure 5 shows the calibration curve and matrix-matched calibration curve. The real-solution calibration was y = 96.048x + 66.084 (R^2 = 0.9981), while the standard-solution calibration was y = 112.58x + 76.936 (R^2 = 0.9983). Substituting the slopes into Eq. (1) gives ME = -14.68%, indicating signal suppression. Because acceptable ME values typically lie within -20% to +20% [26], the observed suppression is within the commonly accepted range, though matrix effects are present and should be noted. Figure 6 presents the SWV which is used to obtain the calibration curve.

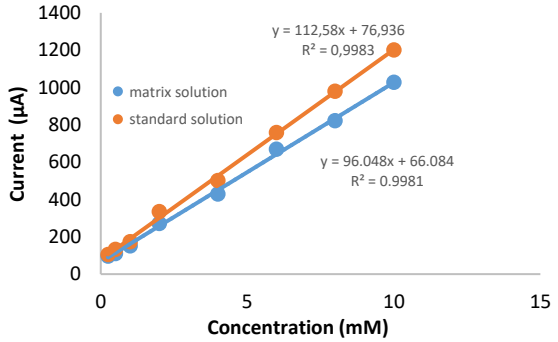

Figure 5. Calibration curves illustrating matrix effects (ME) in fish liver tissue: solvent calibration (orange) compared with matrix-matched calibration (blue).

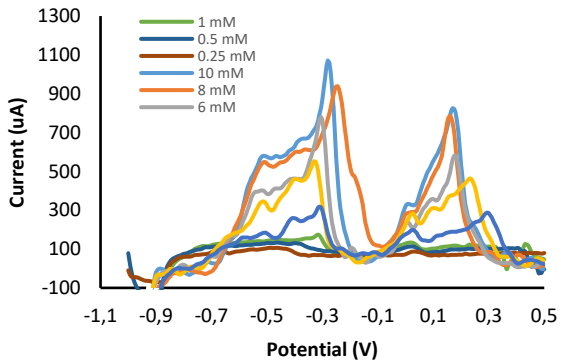

Figure 6. Square-wave voltammograms are used to obtain the calibration curve in standard solutions.

Figure 7 shows the cyclic voltammograms recorded in the presence and absence of Pb(II). In the presence of Pb(II), distinct oxidation and reduction peaks appear, reflecting the characteristic electrochemical response of Pb(II) on the electrode surface. In contrast, the absence of Pb(II) results in a nearly featureless voltammogram, confirming that no significant redox activity occurs in the supporting electrolyte alone.

Figure 8 further corroborates this finding using square-wave voltammetry (SWV). While the blank solution without Pb(II) shows no defined peaks, the addition of 5 mM Pb(II) produces clear current responses, demonstrating the sensitivity of the method toward Pb(II). These consistent results from both CV and SWV confirm that the observed electrochemical signals originate specifically from Pb(II) and not from background interference.

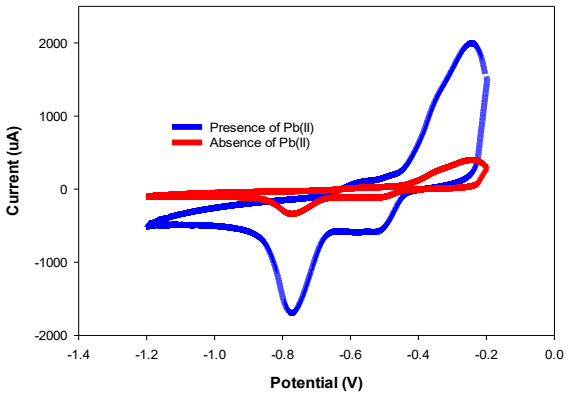

Figure 7. Cyclic voltammograms in the absence and presence of Pb(II)

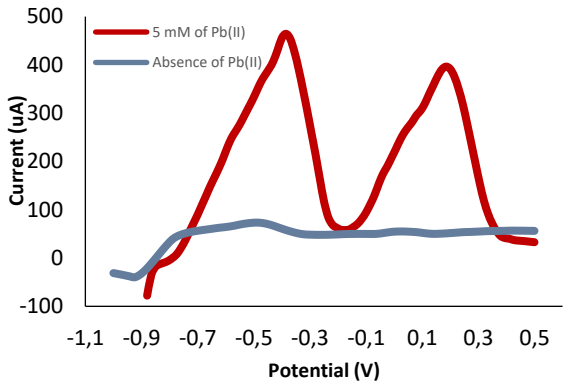

Figure 8. Square-wave voltammograms with and without Pb(II) in 0.1 M KCl

Table 1. The analytical figures of merit for Pb(II).

Linearity [1](mM)	Regression equation	% Recovery	R^2	Limits of detection (mM)	Limits of quantitation (mM)	[2]Precision (%) (ANOVA)	
						Within-day (N=5)	Intermediate precision
0.25-10.0	A= 112.58 [Pb(II)]+76.936	97.16-115.08	0.9983	0.096	0.32	4.1	4.6

[1] Linearity was tested by Mandel test; Concentrations refer to standard solutions in solvent
[2] Precision was calculated by one-way ANOVA

The comparison between the used materials and different magnetic materials for Pb(II) removal/preconcentration is shown in Table 2. Compared to previously reported sensors, the present work introduces a significantly simpler and more accessible approach by employing SPE without any additional surface modifications or nanomaterial enhancements. Despite the absence of functional coatings or composite materials, the sensor successfully detects the target analyte in a complex biological matrix, fish liver, with a LOD of 0.096 mM. This performance, while not the lowest among the listed studies, is particularly notable given the simplicity of the sensor design.

In contrast, other sensors in the literature rely heavily on material-based modifications to enhance sensitivity and selectivity. For instance, Dhaffouli et al. (2024) used a ZnO@SiO_2-APTES-modified glassy carbon electrode (GCE) for water samples, achieving an LOD of 2.6×10^{-5} mM but requiring complex surface functionalization. Similarly, Yao et al. (2024) employed a DMP-Cu composite on GCE, yielding a very low LOD of 3.0×10^{-6} mM and high recoveries, though at the cost of additional material preparation. Other studies, such as Ding et al. (2018) and Luo et al. (2017), utilized nanomaterial-based or polymer-imprinted sensors for detection in environmental or food matrices, demonstrating impressive LODs but involving multi-step fabrication procedures. Even the PA-PPy@SPCE sensor reported by Zhang et al. (2023), which also uses a screen-printed platform, depends on polymer modification to achieve adequate sensitivity.

Table 2. Comparison with other studies

Sensor	Sample	Recovery %	LOD (mM)	Linear range (mM)	pH	Reference
[1]ZnO@SiO_2-APTES/GCE	Tap water, Sea water	88 – 104	2.6×10^{-5}	8.8×10^{-5} - 1.2×10^{-3}	4.6	[27]
[2]DMP-Cu/GCE	Actual tap water, pond water	104.1 – 123.6	3.0×10^{-6}	1.0×10^{-8} - 4.0×10^{-7} 8.0×10^{-7} - 5.0×10^{-5}	5.0	[28]
[3]Au@Ppy/GCE	Polluted soil, baby's nail	-	3.6×10^{-4}	5.0×10^{-7} - 1.0×10^{-5}	7.0	[29]
[4]IIP-CPE	Flour, rice, tap water, Yudai river water	99.1 – 103.7	1.0×10^{-6}	1.0×10^{-6} - 7.5×10^{-4}	5.0	[30]
[5]PA-PPy@SPCE	Tap water	> 93	4.3×10^{-4}	1.0×10^{-5} - 6.0×10^{-4}	5.6	[31]
-	Fish liver	97.16-115.08	9.6×10^{-2}	0.25-10.0	-	Present work

[1]SiO_2-APTES: Amine-functionalized silica-coated zinc oxide nanoparticles, [2]DMP-Cu: 2,5-dimercapto-1,3,4-thiadiazole-functionalized hydroxycopper MOF composite, [3]Au@Ppy: gold nanoparticle–decorated polypyrrole composite, [4]IIP-CPE: lead(II) ion-imprinted polymer modified carbon paste electrode, [5]PA-PPy: phytic acid functionalized polypyrrol

Celal Bayar University Journal of Science
Volume 21, Issue 4, 2025, p 172-181
Doi: 10.18466/cbayarfbe.1718352

Table 3. Pb(II) analysis of fish (*Mugil cephalus*) liver tissue samples with ICP-OES and electrochemically.

Samples	Spike (µg/g)	SPE Found (µg/g) ± SD,	Recovery % ± RSD %,	ICP-OES (µg/g)
1	1036	1046.2 ± 0.89	107.48 ± 0.82	9.49 ± 0.68
2	1036	1054.5 ± 0.36	97.16 ± 0.37	19.04 ± 0.67
3	1036	1038.8 ± 0.50	115.08 ± 0.43	2.44 ± 1.57

3.5. Application of the proposed method with real sample analysis

The proposed general procedure was utilized for the recovery and determination of lead Pb(II) in real samples. To verify the accuracy of the SPE in determining lead concentrations, comparative analysis was performed using ICP-OES. According to the ICP-OES results, lead concentrations in fish (*Mugil cephalus*) liver tissue samples were found to be 9.49, 19.04 and 2.44 µg/g. The SPE was then used to detect lead in three safety liver samples via SWV, and the results were compared to those obtained from ICP-OES to evaluate the sensor's practical applicability and accuracy. The lead concentrations measured by the SPE were 0.25 and 10.00 mM. These measurements were repeated three times under identical conditions. The LOD and LOQ values indicate high precision, and the close agreement between the SPE and ICP-OES results confirms the high accuracy and reliability of the SPE for lead detection in liver samples.

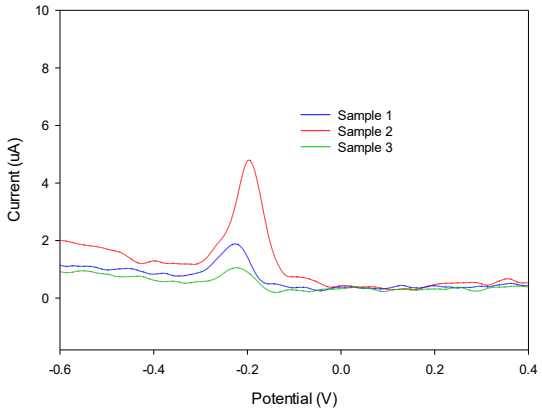

Figure 9. Square wave voltammograms of liver tissue samples (Sample 1: blue, Sample 2: red, Sample 3: green) obtained using the proposed SPE method for Pb(II) detection.

3.6. Selectivity of proposed method

The cyclic voltammetry results presented in the Figure 10 clearly demonstrate the selectivity of the proposed sensor toward Pb(II) ions. As shown, the voltammogram of Pb(II) exhibits a well-defined and intense redox peak within the potential range of approximately –0.6 V to –0.3 V, which is clearly distinguishable from the responses of Zn(II) and Cu(II). In contrast, the Zn(II) and Cu(II) signals are relatively smaller and less pronounced, indicating weaker electrochemical activity under identical experimental conditions. The distinct separation between the Pb(II) peak and those of the other tested metal ions confirms that the electrode surface exhibits a strong affinity and specific redox behavior toward Pb(II). These findings verify that the developed sensor can effectively differentiate Pb(II) from other commonly coexisting bivalent metals such as Zn(II) and Cu(II), minimizing potential interference. Consequently, the results confirm the excellent selectivity and applicability of the sensor for accurate Pb(II) determination in complex biological matrices such as fish liver samples.

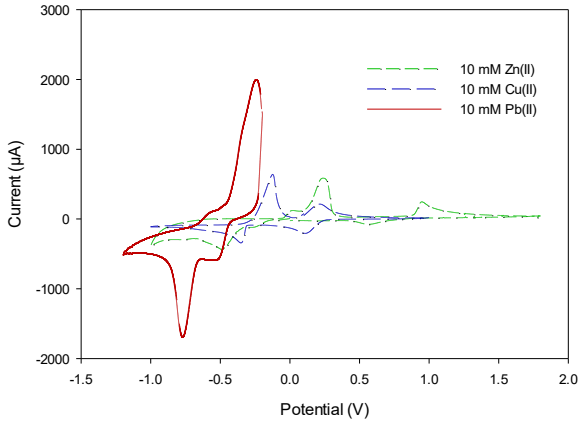

Figure 10. Selectivity of Pb(II) in the presence of other metals.

4. Conclusion

In this study, a straightforward and cost-effective electrochemical method was utilized for the detection of Pb(II) using an unmodified SPE. Through systematic optimization of key experimental parameters, including supporting electrolyte type and concentration, as well as scan rate, 0.1 M KCl and a scan rate of 75 mV/s were identified as optimal conditions, offering enhanced peak

resolution and current response. The method demonstrated good analytical performance, with a wide linear range (0.25–10.0 mM), a low detection limit (0.0096 mM), and high reproducibility, as confirmed by statistical analysis. Notably, the sensor showed strong applicability in fish (*Mugil cephalus*) liver samples, achieving 97.16-115.08% without the need for surface modification or nanomaterial enhancement.

The accuracy of the SPE in determining lead concentrations verified with the comparative analysis of ICP-OES. The close agreement between the SPE and ICP-OES results confirms the high accuracy and reliability of the SPE for lead detection in liver samples. Compared to other reported sensors, this approach offers a simpler yet reliable alternative for lead detection, making it suitable for on-site environmental and food safety monitoring applications.

Acknowledgement

This work did not receive any specific grant from funding agencies in the public, commercial, or not-for-profit sectors.

Author's Contributions

Canan Onac: Drafted and wrote the manuscript, performed the experiment and result analysis.

Ahmet Kaya: Assisted in analytical analysis on the structure, supervised the experiment's progress, result interpretation and helped in manuscript preparation.

Ethics

There are no ethical issues after the publication of this manuscript.

References

[1]. Angon P. B., Islam S.M., Shreejana K.C., Das, A., Anjum, N., Poudel, A., Suchi, S.A. (2024). Sources, effects and present perspectives of heavy metals contamination: Soil, plants and human food chain, *Heliyon,* 10, (7), e28357. (https://doi.org/10.1016/j.heliyon.2024.e28357)

[2]. Lubal M. (2024). Impact of heavy metal pollution on the environment, *Uttar Pradesh Journal of Zoology*, 45(11), 97-105. (10.56557/upjoz/2024/v45i114074)

[3]. Edo G. I., Samuel, P.O., Oloni, G.O., Ezekiel, G.O., Ikpekoro, V.O., Obasohan, P., Ongulu, J., Otunuya, C.F., Opiti, A.R., Ajakaye, R., Essaghah, A.E.A., Agbo, J.J. (2024). Environmental persistence, bioaccumulation, and ecotoxicology of heavy metals, *Chemistry and Ecology,* 40(3), 322-349. (https://doi.org/10.1080/02757540.2024.2306839)

[4]. Kanupuru S. and Kumari, J.P.(2016). Impact of Lead on environment and human health-a review. *World Journal of Pharmaceutical Research*, 5(4), 531-554. (https://doi.org/10.20959/wjpr20164-5913)

[5]. Collin M. S., Venkatraman, S.K., Vijayakumar, N., Kanimozhi, V., Arbaaz, S.M., Stacey, R.G.S., Anusha, J., Choudhary, R., Lvov, V., Tovar, G.I., Senatov, F., Koppala, S., Swamiappan, S. (2022). Bioaccumulation of lead (Pb) and its effects on human: A review, *Journal of Hazardous Materials Advances,* 7, 100094. (https://doi.org/10.1016/j.hazadv.2022.100094)

[6]. Naja G. M., Volesky, B., Jin, X. L., Wang, L. K.(2025). 2 Toxicity and Sources of Pb, Cd, Control of Heavy Metals in the Environment: Recent Advances in Metal Toxicity, Pollution Control, and Remediation Techniques, 29. (https://doi.org/10.1201/9781003541615)

[7]. Varela R. L.(2023). The CDC's updated blood lead reference value and community implications in pediatrics, The Nurse Practitioner, 48(3), 6-9. (https://doi.org/10.1097/01.NPR.0000000000000016)

[8]. Needleman H.(2004). Lead poisoning, *Annu. Rev. Med.,* 55, 209-222. (https://doi.org/10.1146/annurev.med.55.091902.103653)

[9]. Demayo A., Taylor, M. C., Taylor, K. W., Hodson, P. V., Hammond, P. B. (2009). Toxic effects of lead and lead compounds on human health, aquatic life, wildlife plants, and livestock, *Critical Reviews in Environmental Science and Technology,*12(4), 257-305. (https://doi.org/10.1080/10643388209381698)

[10]. Brown M. J. and Margolis, S. (2012). Lead in drinking water and human blood lead levels in the United States. *MMWR Suppl*, 10;61(4):1-9.

[11]. Ravenscroft J., Roy, A., Queirolo, E.I., Manay, N., Martinez, G., Peregalli, F., Kordas, K. (2018). Drinking water lead, iron and zinc concentrations as predictors of blood lead levels and urinary lead excretion in school children from Montevideo, Uruguay, *Chemosphere,* 212, 694-704. (https://doi.org/10.1016/j.chemosphere.2018.07.154)

[12]. EPA U. National Recommended Water Quality Criteria-Aquatic Life Criteria Table. https://19january2021snapshot.epa.gov/wqc/national-recommended-water-quality-criteria-aquatic-life-criteria-table_.html (accessed 5 June 2025, 2024).

[13]. Ariño A., Beltrán, J. A., Herrera, A., Roncalés, P. (2013)."Fish and seafood: Nutritional Value," in Encyclopedia of Human Nutrition (Third Edition), B. Caballero Ed. Waltham: Academic Press, 254-261. (https://doi.org/10.1016/B978-0-12-375083-9.00110-0)

[14]. Phogat S., Dahiya, T. Jangra, M. Kumari, A., Kumar, A. (2022). Nutritional Benefits of Fish Consumption for Humans: A Review, *International Journal of Environment and Climate Change*, 12(12), 1443-1457. (https://doi.org/10.9734/ijecc/2022/v12i121585)

[15]. Almashhadany D. A., Rashid, R. F. Altaif, K. I. Mohammed, S. H. Mohammed, H. I. and Al-Bader, S. M. (2025) Heavy metal(loid) bioaccumulation in fish and its implications for human health, *Italian Journal of Food Science,* 14(1). (https://doi.org/10.4081/ijfs.2024.12782)

[16]. Kaya H., Akbulut, M. (2015). Effects of waterborne lead exposure in Mozambique tilapia: oxidative stress, osmoregulatory responses, and tissue accumulation. *Journal of Aquatic Animal Health*, 27(2), 77-87. (https://doi.org/10.1080/08997659.2014.1001533)

[17]. Yancheva V., Stoyanova, S., Velcheva, I., Georgieva, E. (2020). Fish as indicators for environmental monitoring and health risk assessment regarding aquatic contamination with pesticides, *International Journal of Zoology and Animal Biology*, 3(1), 1-6. (https://doi.org/10.23880/izab-16000210)

[18]. Vallese F. D., Stupniki, S., Trillini, M., Belén, F., Di Nezio, M.S., Juan, A., Pistonesi, M.F. (2024). Bioaccumulation Study of Cadmium and Lead in Cyprinus carpio from the Colorado River, Using Automated Electrochemical Detection, *Water,* 17(77), 1-15. (https://doi.org/10.3390/w17010077)

[19]. Korn M. d. G. A., de Andrade, J. B., de Jesus, D.J., Lemos, V.A., Bandeira, M.L.S.F., dos Santos, W.N.L, Bezerra, M.A., Amorim, F.A.C., Souza, A.S., Ferreira, S.L.C. (2006). Separation and preconcentration procedures for the determination of lead using spectrometric techniques: A review, *Talanta*, 69(1), 16-24. (https://doi.org/10.1016/j.talanta.2005.10.043)

[20]. Zhang N., Peng, Wang, H. S., Hu, B. (2011). Fast and selective magnetic solid phase extraction of trace Cd, Mn and Pb in environmental and biological samples and their determination by ICP-MS*, Microchimica Acta*, 175, 121-128. (https://doi.org/10.1007/s00604-011-0659-3)

[21]. Paul K. B., Kumar, S., Tripathy, S., Vanjari, S. R. K., Singh, V., Singh, S. G. (2016). A highly sensitive self assembled monolayer modified copper doped zinc oxide nanofiber interface for detection of Plasmodium falciparum histidine-rich protein-2: Targeted towards rapid, early diagnosis of malaria, *Biosensors and Bioelectronics*, 15(80), 39-46. (https://doi.org/10.1016/j.bios.2016.01.036)

[22]. Bukkitgar S.D., Shetti, N.P., Malladi, R.S., Reddy, K.R., Kalanur, S. S., Aminabhavi, T. M. (2020.) Novel ruthenium doped TiO2/reduced graphene oxide hybrid as highly selective sensor for the determination of ambroxol, *Journal of Molecular Liquids*, 300, 112368. (https://doi.org/10.1016/j.molliq.2019.112368)

[23]. Kumar S., Vasylieva, N., Singh, V., Hammock, B., Singh, S. G. (2020). A facile, sensitive and rapid sensing platform based on CoZnO for detection of fipronil; an environmental toxin, *Electroanalysis*, 32(9), 2056-2064. (https://doi.org/10.1002/elan.202000051)

[24]. Tunc-Ata M., Akturk, E. Z., Njjar, M., Kaya, A., Akdogan, A., Onac, C. (2025). Determination of retrorsine in thyme via molecularly imprinted electrochemical sensor: Validation and comparison with chromatographic technique, *Food Chemistry*, 418, 144818. (https://doi.org/10.1016/j.foodchem.2025.144818)

[25]. Njjar M., Aktürk, E. Z., Kaya, A., Onac, C., Akdogan, A. (2025). A novel MIP electrochemical sensor based on a CuFe2O4NPs@rGO nanocomposite and its application in breast milk samples for the determination of fipronil, *Analytical Methods*, 17, 5508-5518. (https://doi.org/10.1039/D5AY00911A)

[26]. Ferrer C., Lozano, A., Agüera, A., Girón, A. J., Fernández-Alba, A. R. (2011). Overcoming matrix effects using the dilution approach in multiresidue methods for fruits and vegetables. *Journal of Chromatography A,* 1218(42), 7634-7639. (https://doi.org/10.1016/j.chroma.2011.07.033)

[27]. Dhaffouli A., Salazar-Carballo, P. A., Carinelli, S., Holzinger, M., Barhoumi, H. (2024). Improved electrochemical sensor using functionalized silica nanoparticles (SiO2-APTES) for high selectivity detection of lead ions, *Materials Chemistry and Physics*, 318, 129253. (https://doi.org/10.1016/j.matchemphys.2024.129253)

[28]. Yao C., Wang, H., Zhou, J., Song, W., Rao, Q., Gao, Z., Liu, C., Song, W., Liang, Y. (2024). Exploring a novel, sensitive, and efficient Pb^{2+} electrochemical sensing strategy based on Cu-MOF, *Arabian Journal of Chemistry*, 17, 105498. (https://doi.org/10.1016/j.arabjc.2023.105498)

[29]. Ding J., Liu, Y., Zhang, D., Yu, M., Zhan, X., Zhang, D., Zhou, P. (2018). An electrochemical aptasensor based on gold@ polypyrrole composites for detection of lead ions, *Microchimica Acta*, 13;185(12), 545, 1-7, 2018. (https://doi.org/10.1007/s00604-018-3068-z)

[30]. Luo X., Huang, W., Shi, Q., Xu, W., Luan, Y., Yang, Y., Wang, H., Yang, W. (2017). Electrochemical sensor based on lead ion-imprinted polymer particles for ultra-trace determination of lead ions in different real samples, *RSC Advances*, 7(26), 16033-16040. (https://doi.org/10.1039/C6RA25791G)

[31]. Zhang H., Li,Y., Zhang, Y., Wu, J., Li, S., Li, L.(2023). A disposable electrochemical sensor for lead ion detection based on in situ polymerization of conductive polypyrrole coating, *Journal of Electronic Materials*, 52(3), 1819-1828. (https://doi.org/10.1007/s11664-022-10175-y)